10

Room Temperature Synthesis of ZnO Quantum Dots by Polyol Methods

Rongliang He and Takuya Tsuzuki
Centre for Frontier Materials
Deakin University, Geelong Technology Precinct, Geelong, VIC, Australia

1. Introduction

Zinc oxide is an important semiconducting material having a broad range of applications including transparent conductive oxides (Hosono 2007), ultraviolet (UV) light absorbers (Becheri et al. 2008) and photocatalysts (Beydoun et al. 1999). ZnO nanoparticles exhibit quantum size effects when the particle size is smaller than the exciton-Bohr diameter of ~ 8 nm. In the past, many methods to synthesize ZnO quantum dots were investigated, (Zhang et al. 2010; Xiong et al. 2005; Tang et al. 2009; Tsuzuki & McCormick, 2001). Among them, wet chemical synthesis methods, such as sol-gel, hydrothermal and solvothermal methods, are widely used to obtain free ZnO quantum dots that are detached from substrates. However, this approach normally requires surfactants or capping agents to limit the growth of particles below the exciton-Bohr diameter. This causes some drawbacks such as the necessity to have additional steps in the production process to remove the surfactants from nanoparticles and increased chance of contamination. In addition, wet chemical synthesis of ZnO normally requires high reaction temperatures above 100 ^{o}C. For example, Tang et al. showed that mono-dispersed ZnO quantum dots can be synthesised in triethylene glycol and demonstrated their promising applications in cell labelling, but the reaction required a temperature as high as 280 ^{o}C and stearate acid as a surfactant (Tang et al. 2009). When the high temperatures were not used, the reaction takes a considerable time. Xiong et al. synthesised ZnO quantum dots in triethylene glycol using LiOH and zinc acetate and, although the morphology and optical properties of ZnO was controlled by the molar ratio between LiOH and zinc acetate, this reaction required 30 days to complete at the interface between the air and the polyol solution (Xiong et al. 2011).

This chapter reports a series of novel room-temperature methods to synthesize mono-dispersed ZnO quantum dots in a polyol without using any surfactant additives. Tetraethylene glycol (TEG) was used as the solvent system for the following reasons. TEG is a clear, non-hazardous, inexpensive organic liquid which is miscible with water. TEG has a structural formula of HO-CH_2-CH_2(-O-CH_2-CH_2)$_3$-OH and is sufficiently polar to allow many inexpensive salt raw materials to be dissolved. Hence TEG is more economical than other organic solvents to be used for the synthesis. Furthermore, TEG is reported to have much lower affinity to ZnO surface than PEG or other polar solvents, which is advantageous for the separation of resulting nanoparticles from the solvent phase by simple washing with deionised water (Dobryszycki & Biallozor 2001).

In this research, NaOH and $ZnCl_2$ were used as raw materials and were directly added into TEG without any surfactant additives. In an aqueous environment, $ZnCl_2$ and NaOH normally react readily to form $Zn(OH)_2$ precipitates. However, it was found that the mixture of $ZnCl_2$ and NaOH solutions in TEG did not induce the reaction at room temperature without external energy input. In our previous research (He & Tsuzuki 2010), it was found that, the dissolution speed of the $ZnCl_2$ and NaOH precursors in TEG was quite low at room temperature. Higher temperatures around 60~70 ^oC were necessary to increase the dissolution speed of the precursors. In this study, it was demonstrated that mechanical agitation and UV light irradiation can be used to initiate the reaction to form ZnO quantum dots at room temperature. It was also found that the size of the quantum dots can be tailored by controlling the process parameters, without additional surfactants or capping agents to limit the particle growth.

The details about the effect of process parameters on particle size, physical properties (bandgap, photoluminescence, etc.), and the growth mechanism of ZnO quantum-dots are presented in the following sections.

2. Mechanically induced room temperature synthesis of ZnO quantum dots in TEG

This section describes the activation of the formation of ZnO quantum dots by mechanical milling at room temperature.

2.1 Experimental

In a typical synthesis, 30 ml of tetraethylene glycol (TEG, 99%, Sigma-Aldrich Ltd) was placed in a sealed plastic container with 0.952g $ZnCl_2$ (98%, Fluka, Sigma-Aldrich Ltd., NSW, Australia), 0.56g NaOH pellets (97%, Chem-Supply, SA, Australia) and 10g ZrO_2 milling balls (0.8-1 mm). Then, the precursors were milled for 2 hours using a Spex 8000 mixer/mill to form ZnO quantum dots at room temperature. The prepared quantum dots were sedimented and washed with ethanol using a centrifuge at the speed of 7000 rpm (Eppendorf centrifuge 5417R) until the salinity of the supernatant becomes less than 100 ppm.

The morphology of the ZnO-TEG colloid was studied by transmission electron microscopy (TEM), using a Jeol 2100 microscope with the beam energy of 200 kV. TEM specimen was prepared by evaporating a drop of nanoparticle dispersion on a carbon-coated specimen grid. Particle size distribution was measured by a dynamic light scattering (DLS) method using a Malvern Zetasizer–Nano instrument. UV-vis spectra were obtained using a Varian Cary 3E spectrophotometer. Photoluminescence of ZnO quantum dots was measured using a Varian Cary Eclipse fluorescence spectrometer. For TEM, UV-vis spectroscopy, photoluminescence spectroscopy and DLS measurements, as-prepared ZnO-TEG colloid was used in an diluted form without washing to remove reaction by-products.

The crystal phase and crystallite size were studied by powder X-ray diffraction (XRD) on an X-ray diffractometer (Panalytical X'Pert PRO MRD) with Cu-Kα radiation at a step width of 0.02^o (λ=1.54180 Å). The presence of TEG on the ZnO quantum dots was investigated by Fourier transform infrared spectroscopy (FTIR) using a Bruker Vertex 70 instrument. For XRD and FTIR measurements, washed and dried quantum dots were used.

2.2 Results and discussions

The raw materials, NaOH and $ZnCl_2$ powders, were not readily soluble in TEG at room temperature without mechanical energy input. After the ball milling process, NaOH and $ZnCl_2$ powders were completely dissolved and no sedimentation was observed in the TEG solution. The pH value of the solution was around 8 after 2 hours of milling, which indicated the consumption of OH^- during milling through the reaction between Zn and OH ions. The solution was yellowish and visually transparent. However, when a laser beam was shone onto the as-milled sample, the Tyndall effect was displayed as shown in Figure 1(a), indicative of the presence of quantum dots in the TEG. The bright-field TEM image shown in Figure 1(b) revealed that the size of the synthesized ZnO quantum dots were around 3-5 nm. However, most of the quantum dots appeared to form clusters on the TEM grid. Further high-resolution TEM study shown in Figure 1(c) revealed that the lattice fringes of the particles run in the same direction across the whole structure, indicating that the single quantum dot possessed good crystallinity. Most of the quantum dots were less than 5 nm. The results of particle sizing using the DLS technique support the TEM observation (Figure 1(d)). In the TEG-diluted solution of the as-milled sample, over 90% of the quantum dots were under 5 nm in diameter and average particle size was 3.1 nm.

The crystal structure was also confirmed by XRD (Figure 2) where only the wurtzite phase corresponding to the standard crystallographic data in the JCPDS-ICDD index card No. 36-1451 was observed, indicating that the synthesized powder consisted of a single phase. The crystal size calculated from the diffraction peak broadening using the Scherrer equation was around 4.6 nm, in good agreement with the result of TEM and DLS studies.

The ZnO quantum dots showed significantly high dispersion stability in the TEG solution even after a long aging time; no precipitation was observed after 1 month of aging in the dark environment. In Figure 3(a), it is shown that both fresh and 1-month-aged sample showed identical yellowish colour and transparency. Furthermore, DSL measurements showed that the growth speed of ZnO quantum dots during aging is extremely slow. The particle size increased to only 8-10 nm after 1 month of aging.

It was found that the as-prepared ZnO TEG solution is stable in the glycols but not in water or ethanol. To investigate the dispersion stability of ZnO quantum dots, 30 µl of as-prepared solution was added into 10 ml TEG, ethylene glycol, water and ethanol separately. Then, UV-Vis absorbance measurements were carried out to these diluted ZnO suspensions. In Figure 4, the light scattering effect appeared in the water and ethanol solutions as the higher absorbance values in the visible light range, which indicates the agglomeration of the ZnO quantum dots. However, for the ethylene glycol and TEG solutions, no such absorption or scattering effect was observed in the visible light range, which implies that the quantum dots were well dispersed in the solution without agglomeration.

The absorbance peak position and intensity also varied in the different solutions which revealed the variation of bandgap energy. According to the Tauc's equation, the band gap energy of the nanoparticles can be estimated from the absorbance spectra for direct bandgap semiconductors using the following equation (Tauc et al. 1966):

$$(\alpha h\nu)^2 \propto h\nu - E_g \quad (1),$$

where α is the absorption coefficient, $h\nu$ is the photon energy and Eg is the Tauc optical bandgap energy. By extrapolating the linear portion of the plot $(\alpha h\nu)^2$ versus $h\nu$ to the

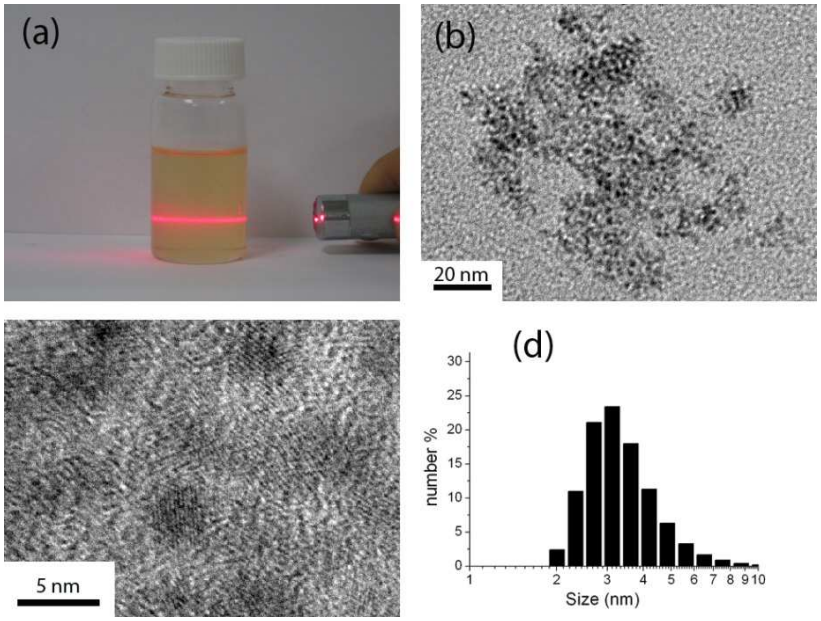

Fig. 1. (a) The Tyndall effect on as-prepared ZnO-TEG solution; (b) bright-field TEM image of as-prepared ZnO; (c) high-resolution TEM image of as-prepared ZnO; (d) size distribution of ZnO in TEG solution.

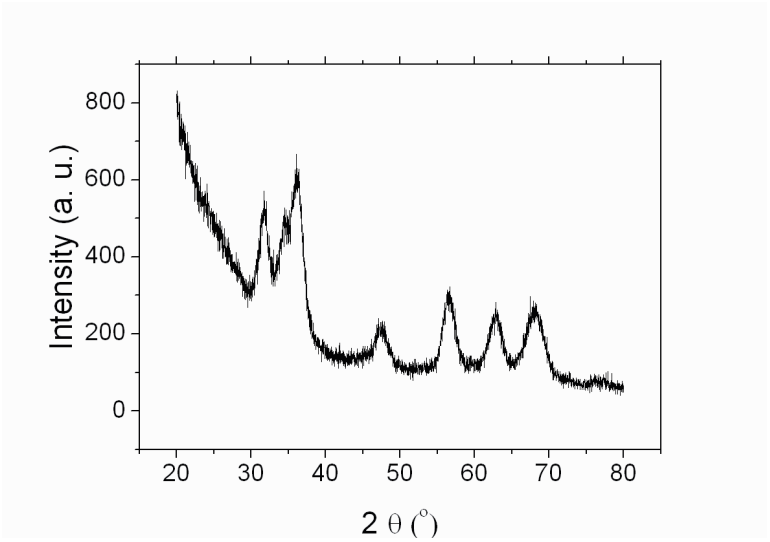

Fig. 2. XRD patterns of washed ZnO.

$(ahv)^2 = 0$ axis, the bandgap value was calculated. The insert graph shows that the band gap of ZnO quantum dots is 3.525 eV in water and 3.556 eV in ethanol. These values are smaller

than that of ZnO in ethylene glycol and TEG (3.636 and 3.644 eV respectively), because of the weakening of the quantum effect due to agglomeration (Tong et al. 2011). The results also support the observation that the as-prepared ZnO quantum dots have high dispersion stability in the polyol medium.

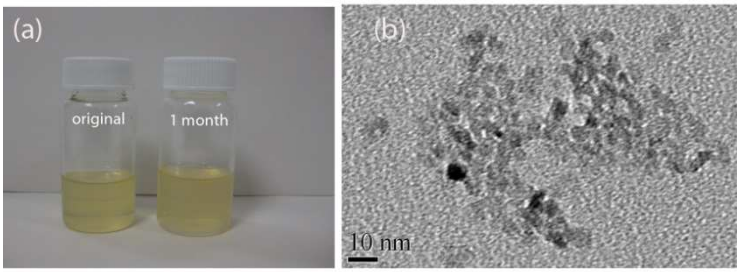

Fig. 3. (a) Appearance of original and 1 month aged ZnO-TEG colloid, and (b) bright-field TEM image of 1 month aged ZnO quantum dots.

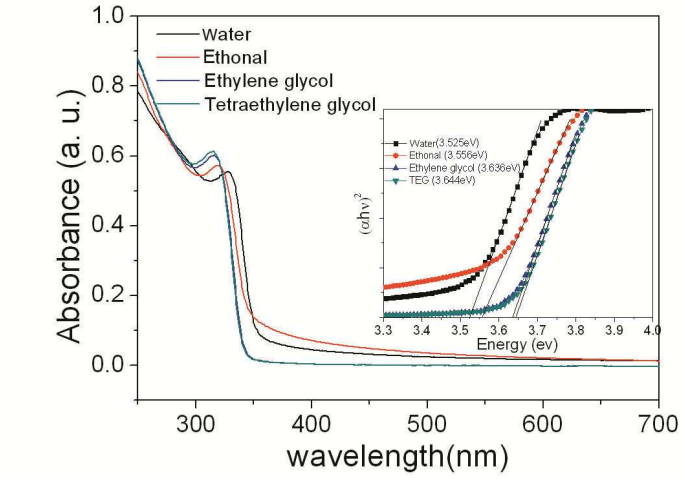

Fig. 4. UV-vis absorbance spectra of ZnO in different solutions. The inset depicts the results of band-gap energy calculation.

The washed sample was also characterized by FTIR to identify the functional groups on the particles to explain its high dispersion stability in TEG. Figure 5 shows FTRI spectra of TEG and washed ZnO quantum dots. The broad peaks at 3420 and 1620 cm^{-1} correspond to the O-H stretching and bending vibrations, respectively, resulting from the presence of hydroxyl groups on the particle surface. The peaks at 2924 and 1384 cm^{-1} are attributed to the unsymmetrical stretching and bending vibrations of $-CH_2$ groups in glycol, respectively. The other characteristic peaks of TEG at 1089.4 and 888.6 cm^{-1} were also present in the spectrum of ZnO nanoparticles (Vafaee & Ghamsari 2007). The results suggest that the ZnO

quantum dots were capped by TEG molecules even after extensive washing with water to remove TEG. The TEG molecules on the surface of quantum dots may provide steric hindrance to provide high stability in polyol solutions such as ethylene glycol and TEG. When the colloid was diluted by water or ethanol, the Van der Waals force would assemble the quantum dots together to exhibit turbidity.

In our previous research (He & Tsuzuki 2010), it was found that, at room temperature, the $ZnCl_2$ and NaOH solutions in TEG did not cause reaction with each other at room temperature and that over 100 °C was required to form ZnO. In order to elucidate the cause of ZnO formation at room temperature by mechanical milling, different amounts of raw materials, that is, a higher concentration (sample A) and a lower concentration (sample B) than the sample described above, were used in this polyol-mechanochemical process as shown in Table 1.

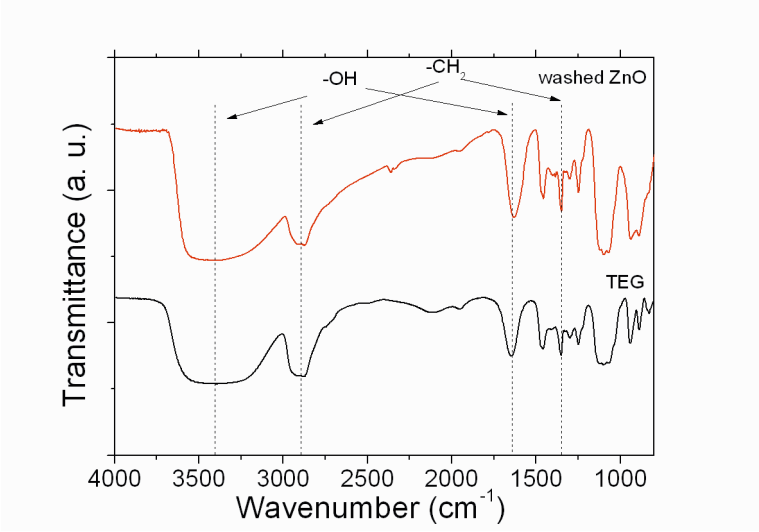

Fig. 5. FT-IR spectra of TEG and washed ZnO.

Sample ID	$ZnCl_2$(g)	NaOH(g)	TEG(ml)
A	1.36	0.8	30
B	0.408	0.24	30

Table 1. Components of raw materials.

After the ball milling process, both solutions of sample A and sample B exhibited a yellowish and transparent appearance. Then, UV-vis absorbance spectra and photo-luminescence spectra were taken on the sample A and sample B (30µl - 10ml) without washing to remove the reaction by-products. Figure 6 shows the UV-vis absorbance spectra of diluted sample A and sample B. It is evident that only sample A has the typical ZnO absorption peak around 340 nm. No absorption peaks can be observed for sample B, indicating that no ZnO quantum dot was synthesised after 2 hours of mechanical

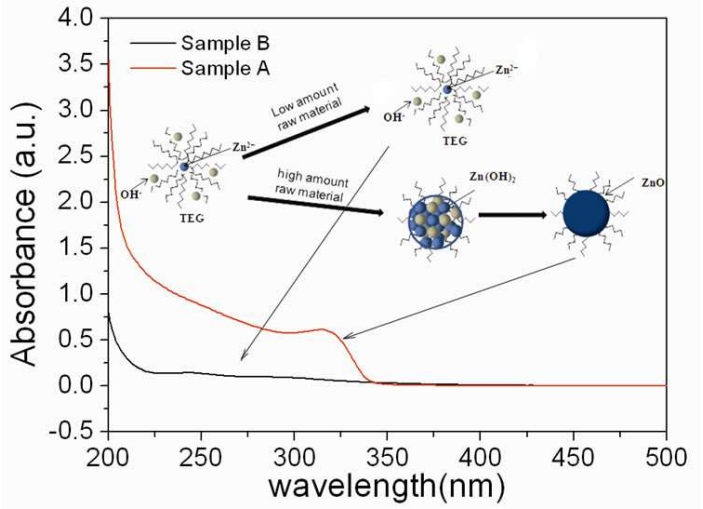

Fig. 6. UV-vis absorbance spectra of diluted sample A and sample B. The inset depicts the reaction process.

milling. Hence, only high concentration of raw materials in the solution resulted in the synthesis of ZnO quantum dots at room temperature using mechanical energy input.

The schematic illustration inserted in Figure 6 gives the possible reaction mechanism involved in the synthesis process. Generally, the hydroxyl groups at both ends of a glycol molecule act as electron donors, giving their lone-pair electrons to those that are electron deficient such as a metal cation, leading to the formation of stable Zn-TEG chelates (Larcher et al. 2003). The formation of stable zinc chelates prevents Zn ions from directly react with OH^- to form $Zn(OH)_2$ at room temperature without other external energy input.

When mechanical energy was introduced to the system, Zn-TEG chelates were de-stabilised and Zn ions are released from the chelates to react with OH^- to form ZnO. When the quantity of raw materials in the TEG solution is lower, the released Zn ions tend to form Zn-TEG chelate again before reacting with OH^-, due to the lesser chance to encounter OH^- in the very close proximity of original Zn-TEG chelates and the strong affinity of TEG to form chelates. This model, however, does not explain why the pH of the as-milled solution of sample B is nearly neutral despite the lack of the formation of ZnO, which is a subject of future study.

In Figure 7, photoluminescence emission spectra of sample A and sample B is shown. Sample A had an emission peak at 525 nm while the emission peak of sample B appeared at 472 nm. The inset photo in Figure 7 shows the difference in the colour of the emitted light, yellow for sample A and blue for sample B. The yellow emission at 500–550 nm was also observed by other research groups who prepared ZnO quantum dots by sol-gel methods (Xiong 2010; Wang et al. 2006; Goharshadi et al. 2011). According to the van Dijiken model, the yellow emission light in sample-A stemmed from the transition of an electron from the conduction band to a deep bandgap level associated with surface defects or oxygen

vacancies (van Dijken et al. 2000). ZnO was not present in sample B. Hence the blue emission the blue emission may have arisen from the Zn-TEG chelates and the photoluminescence may be related to metal assisted ligand-to-ligand charge transfer and an intra-ligand π-π* transition (Gronlund et al. 1995; Bauer et al. 2007), which should be confirmed by further study.

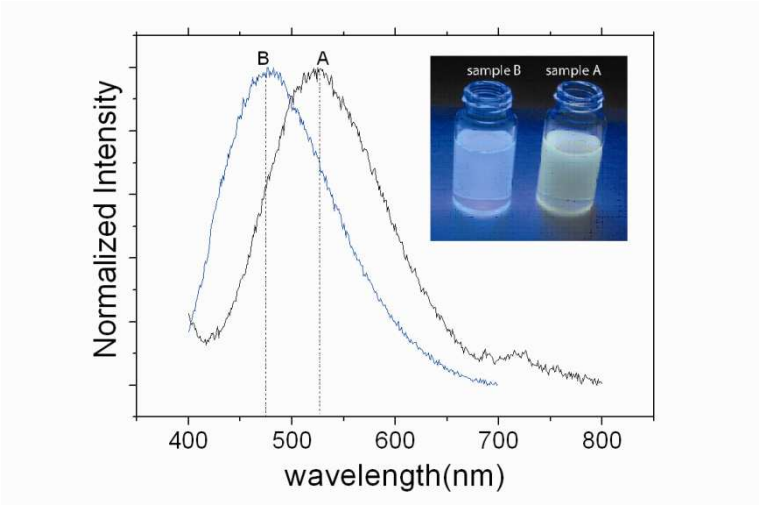

Fig. 7. Photo luminescence emission spectra of diluted sample A and sample B. The inset depicts the colours or emission light under UV light irradiation.

3. UV induced room temperature synthesis of ZnO quantum dots in TEG

This section describes the activation of the formation of ZnO quantum dots by UV irradiation at room temperature.

3.1 Experimental

The synthesis of Zn-TEG chelates was performed firstly by mixing 30 ml of TEG (99%, Sigma-Aldrich Ltd), 0.408g $ZnCl_2$ (98%, Fluka, Sigma-Aldrich Ltd., NSW, Australia), 0.24g NaOH pellets (97%, Chem-Supply, SA, Australia) and 10g ZrO_2 milling balls (0.8-1 mm) together and then ball milling the mixture in a Spex 8000 mixer for 2 hours. This is the same procedure as for preparing the sample B in the previous section. Then, UV-light was irradiated on the as-prepared Zn-TEG chelates solution with continuous stirring in an ice bath. The as-prepared ZnO-TEG colloidal suspension was directly diluted for the characterization by transmission electron microscopy (TEM), UV-vis spectroscopy, photo-luminescence spectroscopy and dynamic light scattering (DLS) measurements.

3.2 Results and discussions

Figure 8 shows the UV-vis absorbance spectra of the solution that was irradiated for up to 8 hours. It is evident that the absorption peak around 300-350 nm gradually appeared when

the exposure time was prolonged over 2 hours, indicative of the formation of ZnO quantum dots. For the sample that was irradiated for 2 hours, the absorption peak appeared at 300 nm which is a much smaller wavelength than that of bulk ZnO. After irradiation for 4 hours, the peak intensity nearly doubled and the peak position was red-shifted to 316 nm, which is attributed to the increase of the number of nucleated ZnO quantum dots and the further growth in particle size. After 8 hours of UV exposure, the peak intensity did not increase much, while the peak position was further red-shifted to 324 nm. The results indicate that the formation of ZnO quantum dots had completed after 4 hours of UV irradiation and that agglomeration or particle growth occurred afterwards. The inserted photo in Figure 8 was taken under UV-light to show the colour of photoluminescence emission. The high intensity of green-yellow emission under UV-light irradiation was an evidence for the presence of ZnO quantum dots and their excellent photoluminescence properties.

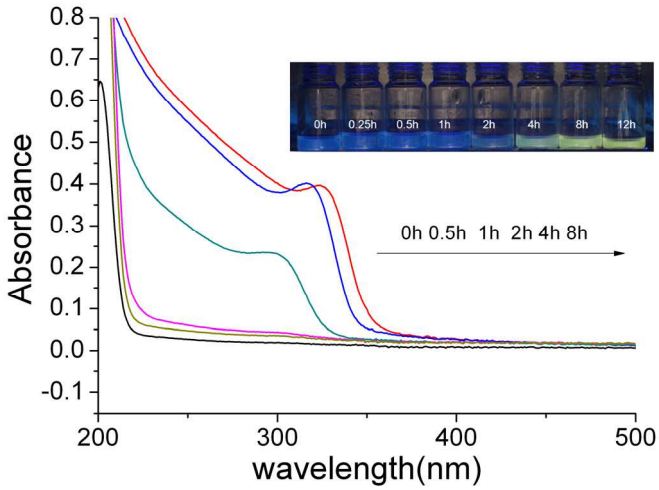

Fig. 8. UV-Vis absorbance spectra of UV-light irradiated TEG solution. The inset depicts the colours of emission light under UV light irradiation.

Because of the strong quantum size effect on the absorption peak energy, the average particle diameter of the ZnO quantum dots can be estimated using the following equation based on the effective mass model (Kumbhakar et al. 2008):

$$d = 2 \times \frac{-0.3049 + \sqrt{-26.23012 + \frac{10240.72}{\lambda_p}}}{-6.3829 + \frac{2483.2}{\lambda_p}} \quad (2),$$

where λ_p is the optical bandgap wavelength. The average diameter thus calculated was 2.6 nm, 3.0 nm and 3.2 nm for the samples irradiated for 2 hours, 4 hours and 8 hours, respectively.

The estimated particle sizes are in good agreement with the sizes observed under TEM (Figure 9). For the sample irradiated for 2 hours, mono-dispersed ZnO nanoparticles were found to have sizes of ~2 nm. These particles had a low contrast in the TEM images against

the carbon film background, possibly due to their low crystallinity. For the sample irradiated for 4 hours, the sizes of primary particles were similar to those of the sample irradiated for 2 hours. However, the image contrast was higher than that of the sample irradiated for 2 hours, implying improved crystallinity. Heavier agglomeration was also found, which may have caused the weakening of quantum size effects and, in turn, the red-shift of the absorption peak.

Although further investigation is necessary to elucidate the mechanism of the UV-light induced room temperature reaction, the possible model is proposed as follows: Firstly, UV-light degrades Zn-TEG chelates to release zinc ions into TEG. It is reported that UV light irradiation can degrade metal chelates to release metal ions (Sun & Pignatello, 1993). Then, the released Zn ions react with OH- ions to form ZnO quantum dots. The newly formed ZnO quantum dots act as a photocatalyst under UV light, by photo-excited electrons and holes creating free radicals when ZnO quantum dots contact with oxygen and water molecules in TEG. The free radicals will decompose the remaining Zn-TEG chelates, releasing more Zn ions to react with OH- ions that increases the number of ZnO quantum dots to be formed. Furthermore, the photo-generated free radicals decompose the TEG on ZnO quantum dots. This weakens the steric hindrance effect of the surface TEG and hence induces particle agglomeration and an increase in crystal size, which results in the red-shift of the optical absorption edge as shown in Figure 8.

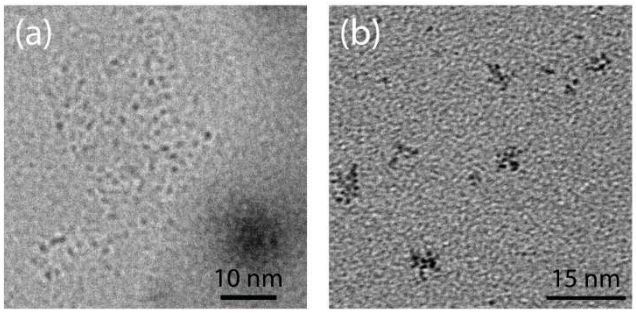

Fig. 9. Bright-field TEM images of ZnO quantum dots synthesized under the UV-irradiation for (a) 2 hours, and (b) 4 hours.

4. Conclusion

In this chapter, novel near-room-temperature methods to synthesize ZnO quantum dots using a polyol were presented. TEG was used as the solvent system in order to enable safe, economical and facile synthesis of free-standing quantum dots. No surfactant or capping agent to limit the particle size growth was added into the reactant mixture. Although $ZnCl_2$ and NaOH can react readily to form $Zn(OH)_2$ precipitates in an aqueous environment, the mixture of $ZnCl_2$ and NaOH solutions in TEG did not induce the reaction at room temperature without external energy input. It was found that mechanical agitation and UV light irradiation can be used to initiate the reaction to form ZnO quantum dots at room temperature. The nanoparticles consisted of ~ 3 - 5 nm sized crystalline primary particles and showed a quantum size effect as a blue-shift of the bandgap energy. It is suggested that

TEG did not only act as a solvent for the reactants but also acted as a surfactant to limit the size of the primary nanoparticles. TEG molecules may bond with ZnO through hydrogen bonding between the –OH group of the surface of ZnO nanoparticles and the –OH terminal of TEG molecules, providing a steric hindrance effect to give high dispersion stability in TEG.

It was proposed that Zn ions form Zn-TEG chelates in TEG and that UV-light irradiation or mechanical milling releases Zn ions from Zn-TEG chelates to form ZnO quantum dots. Further investigation is required to elucidate the reaction mechanism. Extended X-ray absorption fine structure analysis and NMR measurements will allow the conformation of Zn-TEG chelate formation and subsequent release of Zn by UV-irradiation and mechanical milling. The in-depth understanding of the reaction mechanism helps optimise the synthesis conditions to obtain ZnO quantum dots with tailored properties. It is also important to identify the advantages of ZnO quantum dots produced using this method, over the ZnO produced using other methods, in terms of properties and performances in key applications areas such as photocatalysis, gas-sensing, bio-marking and photoluminescence devices.

It is expected that this new synthesis method is applicable for the production of other quantum dots in a safe and scalable manner. In order to further develop the knowledge and techniques on this new method, it is also necessary to investigate the applicability of this method to the synthesis of non-oxide nanoparticles.

5. References

Bauer, C.A.; Timofeeva, T.V.; Settersten, T.B.; Patterson, B.D.; Liu, V.H,; Simmons, B.A. & Allendorf, M.D. (2007). Influence of Connectivity and Porosity on Ligand-Based Luminescence in Zinc Metal−Organic Frameworks. *Journal of the American Chemical Society,* Vol. 129, No. 22, pp. 7136-7144, ISSN 0002-7863

Becheri, A.; Durr, M.; Lo Nostro, P. & Baglioni, P. (2008). Synthesis and characterization of zinc oxide nanoparticles: application to textiles as UV-absorbers. *Journal of Nanoparticle Research,* Vol. 10, No. 4, pp. 679-689, ISSN 1388-0764

Beydoun, D.; Amal, R.; Low, G. & McEvoy, S. (1999). Role of Nanoparticles in Photocatalysis. *Journal of Nanoparticle Research,* Vol. 1, No. 4, pp. 439-458, ISSN 1388-0764

Dobryszycki, J. & Biallozor, S. (2001). On some organic inhibitors of zinc corrosion in alkaline media. *Corrosion Science,* Vol. 43, No. 7, pp. 1309-1319, ISSN 0010-938X

Goharshadi, E.K.; Abareshi, M.; Mehrkhah, R.; Samiee, S.; Moosavi, M.; Youssefi, A. & Nancarrow, P. (2011). Preparation, structural characterization, semiconductor and photoluminescent properties of zinc oxide nanoparticles in a phosphonium-based ionic liquid. *Materials Science in Semiconductor Processing,* Vol. 14, No. 1, pp. 69-72, ISSN 1369-8001

Gronlund, P.J.; Burt, J.A. & Wacholtz, W.F. (1995). Synthesis and characterization of luminescent mixed ligand zinc(II) complexes containing a novel dithiol ligand. *Inorganica Chimica Acta,* Vol. 234, No. 1-2, pp. 13-18, ISSN:0020-1693

He, R.L. & Tsuzuki, T. (2010). Low-Temperature Solvothermal Synthesis of ZnO Quantum Dots. *Journal of the American Ceramic Society,* Vol. 93, No. 8, pp. 2281-2285, ISSN 0002-7820

Hosono, H. (2007). Recent progress in transparent oxide semiconductors: Materials and device application. *Thin Solid Films,* Vol. 515, No. 15, pp. 6000-6014, ISSN 0040-6090

Kumbhakar, P.; Singh, D.; Tiwary, C.S. & Mitra, A.K. (2008). Chemical synthesis and visible photoluminescence emission from monodispersed zno nanoparticles. *Chalcogenide Letters,* Vol. 5, No. 12, pp. 387-394, ISSN 1584-8663

Larcher, D.; Sudant, G.; Patrice, R. & Tarascon, J.M. (2003). Some Insights on the Use of Polyols-Based Metal Alkoxides Powders as Precursors for Tailored Metal-Oxides Particles. *Chemistry of Materials,* Vol. 15, No. 18, pp. 3543-3551, ISSN 0897-4756

Sun, Y.& Pignatello, J.J. (1993). Activation of hydrogen peroxide by iron (III) chelates for abiotic degradation of herbicides and insecticides in water. *Journal of Agricultural and Food Chemistry,* Vol. 41, pp. 308-312.

Tang, X,; Choo, E.S.G.; Li, L.; Ding, J. & Xue, J. (2009). One-Pot Synthesis of Water-Stable ZnO Nanoparticles via a Polyol Hydrolysis Route and Their Cell Labeling Applications. *Langmuir,* Vol. 25, No. 9, pp. 5271-5275, ISSN 0743-7463

Tauc, J.; Grigorovici, R. & Vancu, A. (1966). Optical Properties and Electronic Structure of Amorphous Germanium. P*hysica Status Solidi (b),* Vol. 15, No. 2, pp. 627-637, ISSN 1521-3951

Tong, H.; Umezawa, N. & Ye, J. (2011). Visible light photoactivity from a bonding assembly of titanium oxide nanocrystals. *Chemical Communications,* Vol. 47, No. 14, pp. 4219-4221, ISSN 1359-7345

Tsuzuki, T. & McCormick, P.G. (2001). ZnO nanoparticles synthesised by mechanochemical processing, *Scripta Materialia*, Vol. 44, No. 8-9, pp. 1731-1734. ISSN 1359-6462

Vafaee, M. & Ghamsari, M.S. (2007). Preparation and characterization of ZnO nanoparticles by a novel sol-gel route. *Materials Letters,* Vol. 61, No. 14-15, pp. 3265-3268, ISSN 0167-577X

van Dijken, A.; Meulenkamp, E.A.; Vanmaekelbergh, D. & Meijerink, A. (2000). The kinetics of the radiative and nonradiative processes in nanocrystalline ZnO particles upon photoexcitation. *Journal of Physical Chemistry B,* Vol. 104, No. 8, pp. 1715-1723, ISSN 1089-5647

Wang, Z.L.; Lin, C.K.; Liu, X.M.; Li, G.Z.; Luo, Y.; Quan, Z.W.; Xiang, H.P. & Lin, J. (2006). Tunable photoluminescent and cathodoluminescent properties of ZnO and ZnO : Zn phosphors. *Journal of Physical Chemistry B,* Vol. 110, No. 19, pp. 9469-9476, ISSN 1520-6106

Xiong, H,M,; Liu, D.P.; Xia, Y.Y. & Chen, J.S. (2005). Polyether-Grafted ZnO Nanoparticles with Tunable and Stable Photoluminescence at Room Temperature. *Chemistry of Materials,* Vol. 17, No. 12, pp. 3062-3064, ISSN 0897-4756

Xiong, H.M.; Ma, R.Z.; Wang, S,F, & Xia, Y.Y. (2011), Photoluminescent ZnO nanoparticles synthesized at the interface between air and triethylene glycol. *Journal of Materials Chemistry,* Vol. 21, No. 9, pp. 3178-3182, ISSN 0959-9428

Xiong, H.M. (2010). Photoluminescent ZnO nanoparticles modified by polymers. *Journal of Materials Chemistry,* Vol. 20, No. 21, pp. 4251-4262, ISSN 0959-9428

Zhang, L.; Yin, L.; Wang, C.; Lun, N.; Qi, Y. & Xiang, D. (2010). Origin of Visible Photoluminescence of ZnO Quantum Dots: Defect-Dependent and Size-Dependent. *The Journal of Physical Chemistry C,* Vol. 114, No. 21, pp. 9651-9658, ISSN 1932-7447

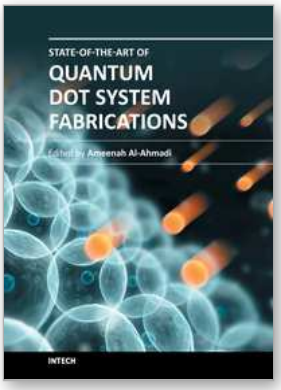

State-of-the-Art of Quantum Dot System Fabrications

Edited by Dr. Ameenah Al-Ahmadi

ISBN 978-953-51-0649-4
Hard cover, 172 pages
Publisher InTech
Published online 13, June, 2012
Published in print edition June, 2012

The book "State-of-the-art of Quantum Dot System Fabrications" contains ten chapters and devotes to some of quantum dot system fabrication methods that considered the dependence of shape, size and composition parameters on growth methods and conditions such as temperature, strain and deposition rates. This is a collaborative book sharing and providing fundamental research such as the one conducted in Physics, Chemistry, Material Science, with a base text that could serve as a reference in research by presenting up-to-date research work on the field of quantum dot systems.

How to reference

In order to correctly reference this scholarly work, feel free to copy and paste the following:

Rongliang He and Takuya Tsuzuki (2012). Room Temperature Synthesis of ZnO Quantum Dots by Polyol Methods, State-of-the-Art of Quantum Dot System Fabrications, Dr. Ameenah Al-Ahmadi (Ed.), ISBN: 978-953-51-0649-4, InTech, Available from: http://www.intechopen.com/books/state-of-the-art-of-quantum-dot-system-fabrications/room-temperature-synthesis-of-zno-quantum-dots-by-polyol-method

INTECH
open science | open minds

InTech Europe
University Campus STeP Ri
Slavka Krautzeka 83/A
51000 Rijeka, Croatia
Phone: +385 (51) 770 447
Fax: +385 (51) 686 166
www.intechopen.com

InTech China
Unit 405, Office Block, Hotel Equatorial Shanghai
No.65, Yan An Road (West), Shanghai, 200040, China
中国上海市延安西路65号上海国际贵都大饭店办公楼405单元
Phone: +86-21-62489820
Fax: +86-21-62489821